DOI: 10.1021/ma9010846

Macromolecules
ARTICLE

Synthesis of Monomeric and Dimeric Copper(II) Carboxylates Bearing Polymerizable Groups and Their Performance in the Copolymerization with MMA

Fatmir Hamza[†] and Guido Kickelbick*[,‡]

[†]*Institute of Materials Chemistry, Vienna University of Technology, Institute of Materials Chemistry, Getreidemarkt 9, 1060 Vienna, Austria, and* [‡]*Saarland University, Inorganic Solid State Chemistry, Am Markt - Zeile 3, 66125 Saarbrücken, Germany*

Received May 18, 2009; Revised Manuscript Received September 1, 2009

ABSTRACT: The formation and characterization of the two binuclear copper(II) carboxylates $Cu_2(L)_4 \cdot 2CH_3OH$ (**1**) and $Cu(L)_2 \cdot H_2O \cdot 2$pyridine (**2**) (L: methacrylate) are described which contain polymerizable groups. The dimeric $Cu_2(L)_4 \cdot 2CH_3OH$ was prepared through reaction of methacrylic acid (LH) with basic copper carbonate in methanol solution. When **1** was dissolved in acetone and pyridine was added in excess to the solution, the binuclear complex turned into the mononuclear complex **2**. **1** and **2** were characterized by UV−vis, IR, and elemental analysis, and the molecular structures were established by single-crystal X-ray diffraction studies. Both complexes were used in copolymerization with methyl methacrylate (MMA). Polymers containing the copper(II) carboxylates were prepared through radical copolymerization of **1** and **2** with MMA using azobis(isobutyronitrile) (AIBN) and benzoyl peroxide (BPO) as initiator. The obtained hybrid polymers were analyzed applying FT-IR, TGA, and size exclusion chromatography. All methods revealed an incorporation of both comonomers in the polymer backbone. Differences in the polymerization kinetics of the compounds can be explained by interactions of the primary initiating radicals with the copper complexes.

Introduction

The combination of polymers with metal complexes can lead to novel hybrid materials[1] which show structures on the molecular length scale that are determined by the type of metal complexes used, their organization in the polymer matrix, and the polymeric backbone. The advantage of the incorporation of metal complexes into polymers is that they can introduce novel properties such as magnetism[2−4] and electronic or optical properties[5] in the final material. The resulting inorganic−organic hybrid composites are thus promising materials for various applications, such as nonlinear optics or energy storage.[6,7] Such polymers can be obtained either using metal complexes with polymerizable groups[8,9] that are copolymerized with regular monomers or by polymers that include functional groups attached to their chain which allow a coordination of metal ions.[10−12] Cross-linked materials are usually obtained if the coordination sites are pending functionalities attached to the polymer chain and metal ions are added to these functionalized polymers. If metal complexes are used as monomers for such structures, they can contain both polymerizable groups and easy accessible coordination sites. An interesting class of metal complexes that fulfill these functions are binuclear metal complexes bridged by carboxylic acids. This type of coordination compound is known to reveal rigid structures with high stability. Generally, they are prepared applying one pot reactions, and in addition the possible metal−metal interactions can induce electronic or magnetic properties into the formed materials.

We present here the synthesis of copper(II) carboxylate complexes bearing polymerizable groups that can be used as building blocks for metal-containing polymers. Copper(II) carboxylate complexes are well-known in the literature, and usually they are prepared either by reaction of the corresponding carboxylic acids with basic copper carbonate or by the reaction of a copper salt with the sodium salt of the carboxylic acid. The complexes present two different reaction sites: a polymerizable bond and a coordination site that is usually saturated with a solvent molecule which can be released by exchange reactions with ligands that show an increased binding affinity (Scheme 1). Polymers containing copper(II) carboxylates were already reported in studies in which the optical properties of copolymers or selective extraction of metal ions into the polymer network were explored.[5,10] However, these previous papers did not investigate the structure of the formed complexes, the morphology of the polymers, or the kinetics of the copolymerization. In this report we will focus on the formation and characterization of two new copper(II) carboxylates $Cu_2(L)_4 \cdot 2CH_3OH$ (**1**) and $Cu(L)_2 \cdot H_2O \cdot 2$pyridine (**2**) and their use as monomers in radical copolymerization with MMA. Copper(II) can undergo reversible one-electron redox reaction with radicals during radical polymerizations, which is extensively used in atom transfer radical polymerization (ATRP) where various copper complexes are employed as catalysts.[13] Hence, the produced monomers offer two different reaction sites for radicals: (i) the polymerizable bond of the methacrylate ligands and (ii) a redox reaction with the copper ion. That makes the polymerization process complex, and the behavior during copolymerization differs compared to other complexes that show only one stable oxidation number such as Ti− and Zr−alkoxides modified with β-keto esters carrying the polymerizable group 2-(methacryloyloxy)ethyl acetoacetate[8] or Zr−carboxylates.[14] In order to understand that behavior, the polymerization was carried out in different ratios of **1**, **2**, and MMA and also with varying amounts of the initiator. The structure and the morphology of the obtained hybrid polymers were investigated using FT-IR, TGA, and size exclusion chromatography (SEC).

Experimental Section

Materials. Methyl methacrylate (Fluka, purum, ≥99.0%) was dried over CaH_2, distilled under argon, and kept at −20 °C.

*Corresponding author. E-mail: kickelbick@mx.uni-saarland.de.

 Published on Web 09/23/2009

All other chemicals were used as received, and solvents were dried with standard procedures and stored under an argon atmosphere.

Measurements. ^{1}H NMR spectra were recorded on a Bruker Avance 300 (^{1}H: 300.13 MHz; ^{13}C: 75.47 MHz) equipped with a 5 mm broadband probe head and a *z*-gradient. Relative size exclusion chromatography (SEC) measurements in tetrahydrofuran were performed using a Waters system including a 515 HPLC pump, a 717 autosampler, a 2410 differential refractive index detector, and Styragel columns (HR0.5, 3, and 4, linear and GPC PHASE SDV 50/100/10E5A) at 40 °C at a rate of 1 mL/min, applying linear polystyrene standards. Molecular weight analyses were carried out using Waters Millennium software including the GPC/V option and related to an internal standard (biphenyl ether).

FT-IR spectra were recorded on a Bruker Tensor 27 instrument working in ATR MicroFocusing MVP-QL with a ZnSe crystal. The software used for analysis was OPUS version 4.0. Elemental analyses were carried out by the Microanalytical Laboratories, University of Vienna. UV−vis spectra were recorded on a Perkin-Elmer Lambda 19 UV/vis spectrometer. TGA was carried out with a Netzsch TG 209c at heating rates of 10 °C min^{-1} in synthetic air, and the data were processed using Netzsch Proteus analysis software.

Scheme 1. Schematic Drawing of a Binuclear Cu(II) Carboxylate with Its Potential Interaction Sites

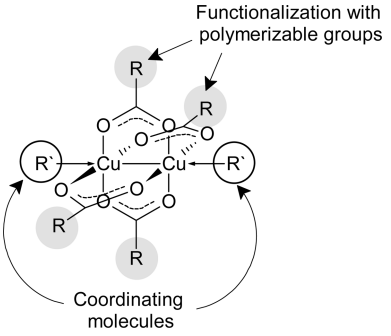

X-ray Diffraction. Selected crystals were mounted on a Bruker-AXS SMART diffractometer with an APEX CCD area detector. Graphite-monochromated Mo K_α radiation (71.073 pm) was used for all measurements. The nominal crystal-to-detector distance was 5.00 cm. A hemisphere of data was collected by a combination of three sets of exposures at 100 or 295 K. Each set had a different ϕ angle for the crystal, and each exposure took 20 s and covered 0.3° in ω. The data were corrected for polarization and Lorentz effects, and an empirical absorption correction (SADABS) was applied. The cell dimensions were refined with all unique reflections. The structures were solved by direct methods (SHELXS97). Refinement was carried out with the full-matrix least-squares method based on F^2 (SHELXL97) with anisotropic thermal parameters for all non-hydrogen atoms. Hydrogen atoms were inserted in calculated positions and refined riding with the corresponding atom. Crystal structure and refinement data are shown in Table 1.

CCDC 728287−728289 contains the supplementary crystallographic data for this paper. These data can be obtained free of charge from the Cambridge Crystallographic Data Centre via www.ccdc.cam.ac.uk/data_request/cif.

Syntheses. *Preparation of $Cu_2(L)_4\cdot 2CH_3OH$ (**1**).* 0.222 g (1 mmol) $Cu_2(OH)_2CO_3$ and 0.528 mL (6 mmol) methacrylic acid were dissolved in 1 mL methanol. The solution was heated under reflux and stirring for 2 h. Then the solution was diluted with 5 mL methanol. After additional heating under reflux for 3 h, the resulting hot mixture was filtered. The methanol and residual acrylic acid were evaporated from the filtered solution under vacuum, and the residue was dissolved in methanol and rested at room temperature for crystallization. Blue-green crystals were obtained after a few days. Yield: 0.419 g (79%). IR: C=C 1643 (m); ν_{as} COO 1590 (vs); ν_s COO 1498 (vs) cm^{-1}. UV−vis: λ_{max} 707.33 nm, λ_{min} 511.92 nm. Elemental anal. calcd for $C_{18}H_{28}Cu_2O_{10}$: C 40.68%, H 5.31%; found: C 39.85%, H 5.09%.

*Preparation of $Cu(L)_2\cdot 2C_5H_5N\cdot H_2O$ (**2**).* Mononuclear Cu-$(OOCCH_3CCH_2)_2\cdot C_5H_5N\cdot H_2O$ was prepared by dissolution of 1.062 g (2 mmol) $Cu_2(L)_4\cdot 2CH_3OH$ in 12 mL hot wet acetone/pyridine 3:1 solution. Blue crystals suitable for XRD measurements were obtained after slow evaporation of acetone. The crystals were filtered off and washed with diethyl ether.

Table 1. Crystal Data and Structure Refinement for $Cu_2(L)_4\cdot 2CH_3OH$ (1), $Cu(L)_2\cdot 2C_5H_5N\cdot H_2O$ (2), and $Cu_2(OOCC_6H_5)_4\cdot 2CH_3CH_2OH$ (3)

empirical formula	$Cu_2(OOCCH_3CCH_2)_4\cdot 2CH_3OH$ $C_{18}H_{28}Cu_2O_{10}$	$Cu(OOCCH_3CCH_2)_2\cdot 2C_5H_5N\cdot H_2O$ $C_{18}H_{22}CuN_2O_5$	$Cu_2(OOCC_6H_5)_4\cdot 2CH_3CH_2OH$ $C_{32}H_{32}Cu_2O_{10}$
formula weight	531.48	409.92	703.66
crystal system, space group	monoclinic, *C*2/*c*	orthorhombic, *Fdd*2	monoclinic, *C*2/*c*
unit cell dimensions [pm, deg]	a = 3740.3(8), α = 90 b = 696.52(1), β = 97.15 c = 1884.7(4), γ = 90	1538.95(10), α = 90 4077.1(2), β = 90 589.56(3), γ = 90	4730.7(5), α = 90 668.23(7), β = 113.43 2206.5(2), γ = 90
temperatur (K)	295(2)	100(2)	295(2)
volume [×10^6 pm^3]	4871.8(1)	3699.2(4)	6400.2(1)
Z, calcd density [mg cm^{-3}]	8, 1.449	8, 1.472	8, 1.461
absorption coefficient [mm^{-1}]	1.791	1.212	1.384
F(000)	2192	1704	2896
crystal size [mm]	0.49 × 0.41 × 0.34	0.41 × 0.33 × 0.28	0.39 × 0.37 × 0.29
θ range for data collection [deg]	2.31−25.00	2.83−25.00	2.54−25.00
limiting indices	$-44 \le h \le 43$ $-8 \le k \le 8$ $-13 \le l \le 22$	$-18 \le h \le 18$ $-48 \le k \le 48$ $-6 \le l \le 6$	$-56 \le h \le 32$ $-7 \le k \le 7$ $-23 \le l \le 26$
reflections collected/unique	12679/4279 [*R*(int) = 0.0281]	6868/1615 [*R*(int) = 0.0416]	16454/5623 [*R*(int) = 0.0657]
completeness to θ = 25 [%]	99.6	99.8	99.9
max and min transmission	0.5810 and 0.4739	0.7278 and 0.6364	0.6143 and 0.6897
data/restraints/parameters	4289/0/285	1614/1/121	5623/0/407
goodness-of-fit on F^2	1.07	1.059	0.905
final *R* indices [$I > 2\sigma(I)$]	R_1 = 0.0407, wR_2 = 0.1048[a]	R_1 = 0.0199, wR_2 = 0.0541[b]	R_1 = 0.0425, wR_2 = 0.0965[c]
R indices (all data)	R_1 = 0.0497, wR_2 = 0.1081[a]	R_1 = 0.0202, wR_2 = 0.0542[b]	R_1 = 0.0658, wR_2 = 0.1014[c]
largest diff peak and hole [e Å^{-3}]	0.31 and −0.271	0.273 and −0.273	0.535 and −0.350

[a] Weight = $1/[\sigma^2(F_o^2) + (xP)^2 + yP]$, where $P = (\mathrm{Max}(F_o^2, 0) + 2F_c^2)/3$, x = 0.0516, and y = 9.43. [b] Weight = $1/[\sigma^2(F_o^2) + (xP)^2 + yP]$, where $P = (\mathrm{Max}(F_o^2, 0) + 2F_c^2)/3$, x = 0.0324, and y = 2.58. [c] Weight = $1/[\sigma^2(F_o^2) + (xP)^2 + yP]$, where $P = (\mathrm{Max}(F_o^2, 0) + 2F_c^2)/3$, x = 0.0516, and y = 0.00.

Scheme 2. Synthesis of $Cu_2(L)_4 \cdot 2CH_3OH$

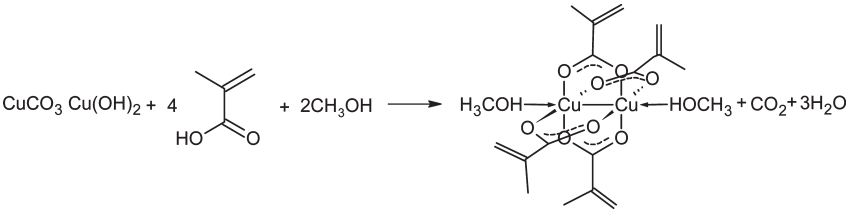

Yield: 1.22 g (71%). IR: C=C 1641 (m); ν_{as} COO 1578−1565 (vs); ν_s COO 1374 (vs) cm^{-1}. Elemental anal. calcd for $C_{18}H_{22}CuN_2O_5$: C 52.74%, H 5.41%, N 6.83%; found: C 52.30%, H 5.26%, N 6.74%.

Preparation of $Cu_2(OOCC_6H_6)_4 \cdot 2CH_3CH_2OH$. 0.531 g (1 mmol) $Cu_2(L)_4 \cdot 2CH_3OH$ and 0.484 g (2 mmol) benzoyl peroxide were dissolved in 10 mL of 1:1 ethanol/toluene solution. The solution was heated under reflux and stirring for 12 h and rested at room temperature for crystallization. Blue-green crystals of $Cu_2(OOCC_6H_6)_4 \cdot 2CH_3CH_2OH$ were obtained after a few days. The crystals were filtered off and washed with a small amount of ethanol. Yield 0.48 g (68%). Elemental anal. calcd for $C_{32}H_{32}Cu_2O_{10}$: C 54.62%, H 4.58%; found: C 54.15%, H 4.59%.

Copolymerization. *Copolymerization of MMA with $Cu_2(L)_4 \cdot 2CH_3OH$ and AIBN as Initiator.* A dry glass tube was charged with (0.5, 0.35, 0.22, 0.1, 0.02, 0.01, 0.005 g) (0.95, 0.65, 0.41, 0.19, 0.038, 0.018, 0.009 mmol) $Cu_2(L)_4 \cdot 2CH_3OH$ and 0.01 g, (0.06 mmol) AIBN and closed by a septum, and the mixture was degassed by three vacuum−argon cycles and sealed under argon. 2 mL (0.0187 mmol) MMA were added to this mixture through a syringe. The tube was placed in an oil bath heated at 85 °C for 12 h. After finishing the polymerization, the reaction mixture was dissolved in THF and added dropwise into methanol. Subsequently, the precipitated polymer was filtered off, washed three times with methanol, and dried under vacuum.

Copolymerization of MMA with $Cu_2(L)_4 \cdot 2CH_3OH$ and BPO as Initiator. A dry glass tube was charged with (0.5, 0.1, 0.02 g) (0.95, 0.19, 0.038 mmol) $Cu_2(L)_4 \cdot 2CH_3OH$ and 0.02g (0.082 mmol) BPO and closed by a septum, and the mixture was degassed by three vacuum−argon cycles and sealed under argon. Two milliliters (0.0187 mmol) MMA were added to this mixture through a syringe. The tube was placed in an oil and heated at 70 °C for 12 h. After finishing the polymerization, the reaction mixture was dissolved in THF and added dropwise into methanol. Subsequently, the precipitated polymer was filtered off, washed three times with methanol, and dried under vacuum.

Copolymerization of MMA with $Cu(L)_2 \cdot 2C_5H_5N \cdot H_2O$. A dry glass tube was charged with (0.5, 0.22, 0.1, 0.02, 0.01 0.005 g) (1.17, 0.515, 0.234, 0.046, 0.023 0.011 mmol) $Cu(L)_2 \cdot 2C5H5N \cdot H_2O$ and 0.02 g (0.082 mmol) BPO and closed by a septum. The mixture was degassed by three vacuum−argon cycles and sealed under argon. 2 mL (0.0187 mmol) MMA were added to this mixture through a syringe. The tube was placed in an oil bath and heated at 75 °C for 12 h. After finishing the polymerization, the reaction mixture was dissolved in THF and added dropwise into methanol. Subsequently, the precipitated polymer was filtered off, washed three times with methanol, and dried under vacuum.

Copolymerization with Variation of Initiator Concentration. A dry glass tube was charged with (0.02 g, 0.037 202 mmol) $Cu_2(L)_4 \cdot 2CH_3OH$ and (0.02, 0.015, 0.01, 0.001 g)(0.12, 0.09, 0.06, 0.006 mmol) AIBN closed by a septum. The mixture was degassed by three vacuum−argon cycles and sealed under argon. 2 mL (0.0187 mmol) MMA were added to this mixture through a syringe. The tube was placed in an oil bath heated at 85 °C for 12 h. After finishing the polymerization, the reaction mixture was dissolved in THF and added dropwise into methanol. Subsequently, the precipitated polymer was filtered off, washed three times with methanol, and dried under vacuum.

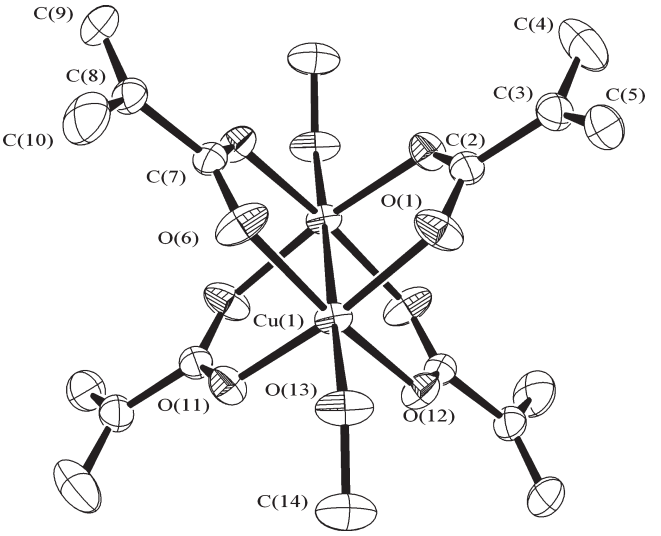

Figure 1. ORTEP view of the structure of complex **1** displaying the thermal ellipsoids at 30% probability. H atoms are omitted for clarity.

Results and Discussion

Synthesis of Copper(II) Carboxylates. Copper(II) carboxylates are usually prepared either by reaction of carboxylic acids with basic copper carbonate[15] or by the reactions of the copper salts with carboxylic acid. $Cu_2(L)_4 \cdot 2CH_3OH$ was synthesized through reaction of methacrylic acid with basic copper carbonate in methanol solution, and the green prismatic crystals suitable for single crystal X-ray diffraction measurements were obtained through recrystallization from methanol (Scheme 2). Crystals of $Cu_2(L)_4 \cdot 2CH_3OH$ are unstable in air because they lose methanol over time.

One feature of the IR data of these compounds is the separation between $\nu_{as}(COO^-)$ and $\nu_s(COO^-)$, which has often been used to diagnose the coordination modes of carboxylate ligands. The IR spectrum of **1** showed a strong peak at 1590 cm^{-1} which corresponds to the $\nu_{as}(COO^-)$ vibration, and the other observed at 1498 cm^{-1} is attributed to the $\nu_s(COO^-)$ stretching vibration.[16] The separation for monodentate carboxylate groups is >200 cm^{-1}, whereas it is <200 cm^{-1} in bidentate groups.[17] The separation between $\nu_{as}(COO^-)$ and $\nu_s(COO^-)$ for **1** is 194 cm^{-1}, indicating a bidentate coordination mode for coordinated carboxylate groups. This result is supported by the single-crystal X-ray analysis.

The unit cell of **1** contains two independent binuclear complexes, each with inversion symmetry (Figure 1). Crystal data and structure refinement for **1** are summarized in Table 1. In each dimer, two copper atoms are bridged by four methacrylate groups, forming a cage structure, as normally found in adducts of copper(II) acetate, and the methanol ligands are bonded through their oxygen atoms to the copper atoms in the axial positions. Selected bond distances and angles of complex **1** are listed in Table 2. Each copper center has a distorted octahedral coordination geometry generated by four oxygen atoms of the carboxylate

groups from different ligands (average Cu−O length: 195.9(3) pm) and one oxygen atom from a methanol ligand. As expected, the Cu−O bond lengths of the methanol ligands (212.8(4), 212.9 (4) pm) are significantly longer than that of those generated by the carboxylates. The bond angles around the Cu center deviate only slightly from 90° or 180°. The Cu(1)−Cu(1) distance in **1** is 258.8(9) pm, which is shorter than the Cu−Cu distance of 264 pm in copper(II) acetate.[18] In the crystal a one-dimensional structure is formed by intermolecular hydrogen bonds. The O(13)−H(13) group from methanol is involved in the formation of an intermolecular bond (O−H···O, 304.1(7) pm) with the carbonyl oxygen O(1) atom of a neighboring molecule (Figure 2).

Exchange reactions of the coordinated solvent molecules are a potential pathway for a further derivatization of the copper complexes. When an excess of pyridine in relation to the existing methanol ligands was added to a solution of **1** in wet acetone, the color of the solution changed from green to blue, which was an indication of the exchange reaction.

The IR spectrum of the obtained compound **2** showed a wide band at about 3200 cm^{-1}, which can be assigned to ν(O−H) stretching and weak signals in the region of C=C stretching at 1641 cm^{-1}. The band assigned as $\nu_{as}(COO^{-})$ splits into two partially overlapping bands 1578−1565 cm^{-1}, and the band observed at 1374 cm^{-1} is attributed to the $\nu_s(COO^{-})$ stretching vibration. Compared to **1** the separation between $\nu_{as}(COO^{-})$ and $\nu_s(COO^{-})$ only increases slightly. It was shown that the occurrence of hydrogen bonding between the noncoordinated oxygen atom of a unidentate carboxylate ligand may give a "pseudo-bridging" arrangement.[19] In that case, the unidentate carboxyl group retains the symmetrical structure.

Crystals suitable for single-crystal X-ray diffraction analysis were obtained after slow evaporation of acetone. Blue crystals of **2** are unstable in air because they lose pyridine over time, and their color turned to green, which reflects the formation of binuclear species.[20] The crystal structure of $Cu(OOCCH_3CCH_2)_2 \cdot 2C_5H_5N \cdot H_2O$ consists of mononuclear units and is shown in Figure 3. Crystal data and structure refinement for **2** are summarized in Table 1. Selected bond lengths and angles are presented in Table 3. The molecular structure of the formed product revealed that the binuclear copper complex rearranged to a mononuclear complex with a square-pyramidal coordination geometry (Scheme 3). The two pyridine nitrogen atoms and two carboxylate oxygen (Cu−O length: 193.76(1) pm) atoms from methacrylate form a tetrahedrally distorted basal square plane. The apical site is occupied by a water molecule and is perpendicular to the basal plane. The distances Cu−O 193.76 (1) pm, Cu−N 201.79(1) pm, and Cu−OH_2 224.7(2) pm are comparable with those found for aquabis(crotonato)bis(pyridine)copper(II)[21] and aquabis(nonanoato)bis(pyridine)copper(II).[19] The oxygens from carboxylates O(4) and O(4^{i}) are not coordinated to copper but interact with water from a neighboring molecule by

Table 2. Selected Bond Lengths [pm] and Angles [deg] for $Cu_2(L)_4 \cdot 2CH_3OH$ (1)[a]

Cu(1)−O(12)	194.6(2)	O(11)−Cu(1)−O(1)	168.58(1)
Cu(1)−O(11)	195.6(3)	O(6)−Cu(1)−O(1)	88.16(1)
Cu(1)−O(6)	196.1(3)	O(12)−Cu(1)−O(1)	95.63(1)
Cu(1)−O(1)	196.6(3)	O(11)−Cu(1)−O(1)	95.80(1)
Cu(1)−O(13)	212.3(4)	O(6)−Cu(1)−O(1)	95.61(1)
Cu(1)−Cu(1)#1	258.89(9)	O(1)−Cu(1)−O(1)	95.48(1)
		O(12)−Cu(1)−Cu(1)#1	84.10(8)
O(12)−Cu(1)−O(11)	90.89(1)	O(11)−Cu(1)−Cu(1)#1	84.92(9)
O(12)−Cu(1)−O(6)	168.71(1)	O(6)−Cu(1)−Cu(1)#1	84.65(9)
O(11)−Cu(1)−O(6)	88.99(1)	O(1)−Cu(1)−Cu(1)#1	83.81(9)
O(12)−Cu(1)−O(1)	89.75(1)		

[a] Symmetry transformations used to generate equivalent atoms: #1 $-x+1, -y+2, -z+1$.

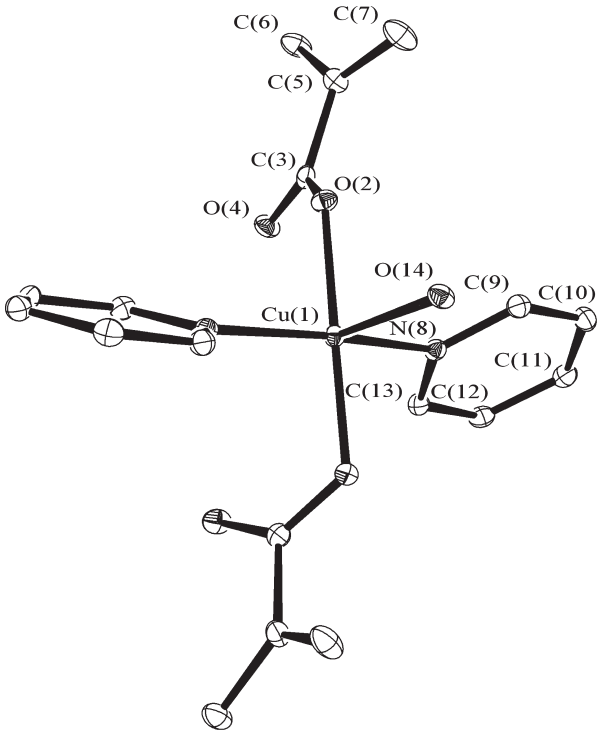

Figure 3. ORTEP view of the structure of complex **2**, displaying the thermal ellipsoids at 30% probability. H atoms are omitted for clarity.

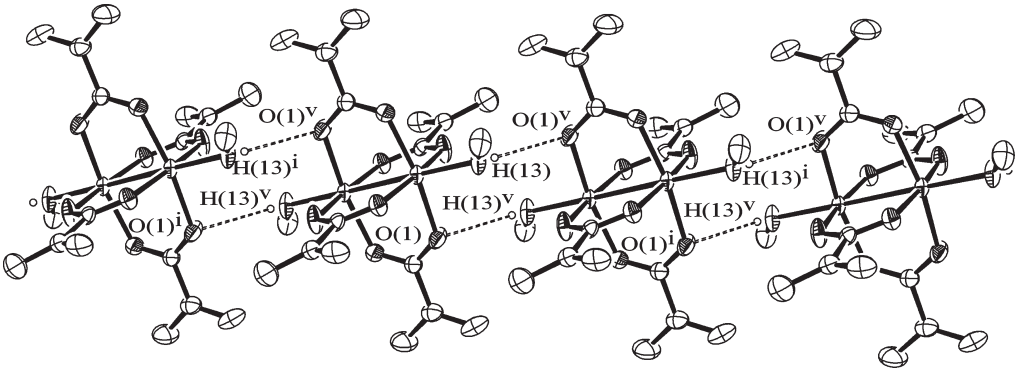

Figure 2. One-dimensional structure of **1**. Dashed lines indicate hydrogen bonds.

Scheme 3. Synthesis of $Cu(OOCCH_3CCH_2)_2 \cdot 2C_5H_5N \cdot H_2O$

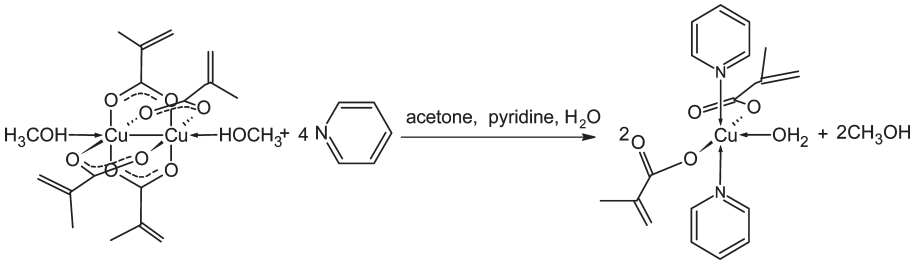

Table 3. Selected Bond Lengths [pm] and Angles [deg] for $Cu(OOCCH_3CCH_2)_2 \cdot 2C_5H_5N \cdot H_2O$ (2)[a]

Cu(1)−O(2)#1	193.76(1)	O(2)−Cu(1)−N(8)#1	90.81(5)
Cu(1)−O(2)	193.76(1)	O(2)#1−Cu(1)−N(8)	90.81(5)
Cu(1)−N(8)#1	201.79(1)	O(2)−Cu(1)−N(8)	89.29(5)
Cu(1)−N(8)	201.79(1)	N(8)#1−Cu(1)−N(8)	167.42(9)
Cu(1)−O(14)	224.7(2)	O(2)#1−Cu(1)−O(14)	89.58(5)
		O(2)−Cu(1)−O(14)	89.58(5)
O(2)#1−Cu(1)−O(2)	179.15(9)	N(8)#1−Cu(1)−O(14)	96.29(5)
O(2)#1−Cu(1)−N(8)#1	89.29(5)	N(8)−Cu(1)−O(14)	96.29(5)

[a] Symmetry transformations used to generate equivalent atoms: #1 $-x + {}^3/_2, -y + {}^1/_2, z$.

hydrogen bonds (276.99(1) pm) to form a one-dimensional structure (Figure 4).

Synthesis of Copolymers. The obtained complexes were used as monomers in the preparation of metal-containing polymers. The reaction behavior of the dimeric copper(II) methacrylates as monomers was systematically studied in free radical copolymerizations with MMA. The inorganic−organic hybrid materials were prepared through a radical polymerization of **1** and **2** with MMA using azobis(isobutyronitrile) (AIBN) and benzoyl peroxide (BPO) as initiators. Previous studies revealed that the copolymerization of Zr- and Ti-containing metal complexes bearing more than one polymerizable group with MMA leads to cross-linked insoluble polymers.[8,14] Contrarily, the copolymerization of copper(II) methacrylates **1** and **2** leads to the formation of soluble copolymers and copolymers with lower molecular weight compared to the literature reported examples.

Copolymerization of MMA with **1** using AIBN as initiator was carried out in a dry glass tube in different ratios (0.95, 0.65, 0.41, 0.19, 0.038, 0.018, 0.009 mmol) of **1** with 0.06 mmol (0.01 g) AIBN as initiator. MMA was added to this mixture, and the polymerization was stopped after heating at 85 °C for 12 h. The elapsed time up to reaching the gel point in the polymerization was indirectly proportional to the concentration of complex **1** in solution. The samples with highest concentration of **1** (0.95, 0.65 mmol) did not result in a solid product even after 12 h. The reaction mixtures of these polymerizations were viscous liquids, which after removing residual MMA and **1** became blue powders. The lower viscosity is an indication that only short polymer chains were formed. All copolymers were soluble in THF which is an evidence that the copolymers are not or only slightly cross-linked. Residual copper(II) carboxylate and MMA were removed from the reaction mixture by dissolving the polymer in THF in addition to the precipitation of the dissolved polymer in methanol. Copper(II) carboxylate and MMA are soluble in a methanol/THF mixture while the copolymer is insoluble. Molecular weight and molecular weight distribution of these samples were determined by SEC (Table 4).

Generally, as shown in Table 4, an increasing amount of **1** resulted in lower molecular weights of the polymers. Copolymers obtained from samples with 0.95 and 0.65 mmol of **1** have the lowest molecular weights and conversion, but the molecular weight distributions are not as broad as for other samples (Figure 5). The samples with 0.018 and 0.009 mmol of **1** showed the highest molecular weights and the broadest molecular weight distributions. Figure 6 shows the dependence of the molecular weight and molecular weight distribution on the concentration of **1** during copolymerization. It can be concluded that the influence of **1** to the polymerization process is high and that the molecular weight and molecular weight distribution are controlled by the amount of copper complex in the reaction mixture. An increasing amount of **1** in the reaction mixture indicates formation of copolymers with decreasing molecular weights. In addition, the conversion decreases with increasing concentration of **1** as shown in Figure 7. A conclusion from these results is that complex **1** inhibits polymerization at higher concentrations by deactivation of radicals from propagating chain. For that reason the conversion of samples with higher concentration of **1** is low and the molecular weight of these copolymers is also quite low. Reduced concentrations of complex **1** produce slightly cross-linked products and hence increase the experimental molecular weight.

Copolymerization of MMA with **1** using BPO as initiator was carried out applying the same procedure that was used for the preparation of samples initiated with AIBN. The difference between AIBN and BPO, besides their different reactivity, is that AIBN produces carbon-centered radicals whereas BPO results in oxygen-centered ones. All copolymers produced, using BPO as initiator, were again soluble in THF. Similar to the previous results, this shows that the copolymers are not or only slightly cross-linked. The behavior concerning the gelation point follows the same systematic with regard to the concentration of the complex as in the case of AIBN: the sample with lowest concentration of **1** (0.038 mmol) reaches the gelation point at the earliest point, and an increasing concentration leads to incomplete conversion of the polymers after 12 h reaction time. Molecular weight and molecular weight distribution of these samples have been determined by SEC analysis. The results are summarized in Table 5. The sample with 0.95 mmol of **1** has the lowest molecular weight, but the molecular weight distribution is not as broad as for other samples. The samples with 0.038 and 0.19 mmol of **1** show higher molecular weights and broader molecular weight distributions. Figure 8 shows that the experimental molecular weight of the copolymers decreases with increasing concentration of **1** in the reaction mixture.

Thus, in both polymerization processes initiated with AIBN and BPO an increasing amount of **1** in the reaction mixture produced lower molecular weights and also lower conversion. Hence, it can be concluded that the behavior of copolymerization initiated with BPO does not differ significantly from copolymerization initiated with AIBN.

The copper complexes can play a role in redox reactions with the propagating radicals in the polymerization reactions

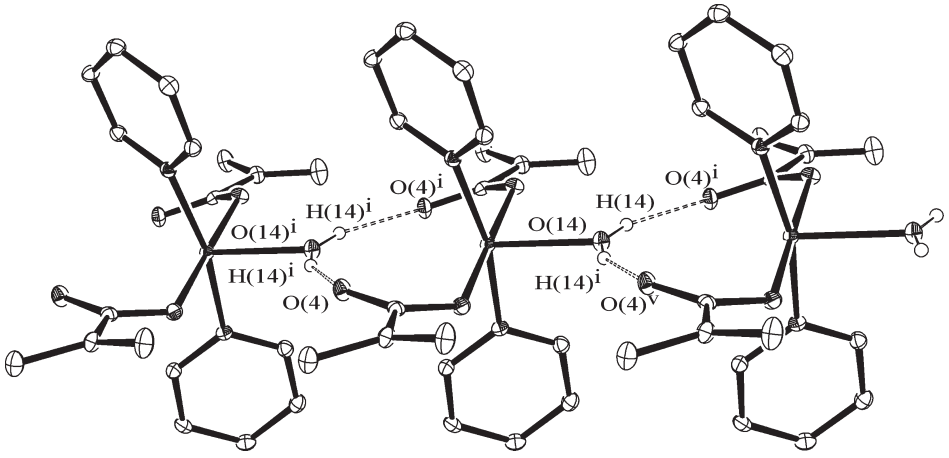

Figure 4. One-dimensional structure of **2**. Dashed lines indicate hydrogen bonds.

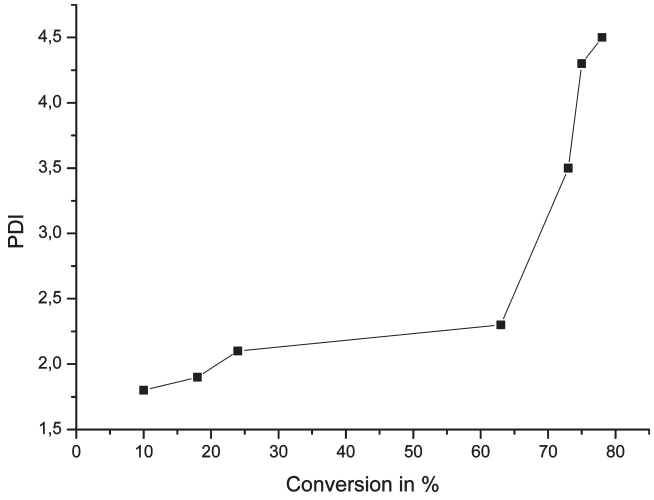

Figure 5. PDI related to conversion during radical copolymerization of MMA with $Cu_2(L)_4 \cdot 2CH_3OH$ initiated with AIBN at 85 °C.

Table 4. Radical Copolymerization of MMA with $Cu_2(L)_4 \cdot 2CH_3OH$ in Bulk Initiated with AIBN at 85 °C

$Cu_2(L)_4 \cdot 2CH_3OH$ (mmol)	MMA (mol)	AIBN (mmol)	yield (%)	M_w ($\times 10^3$)	M_n ($\times 10^3$)	PDI
0.95	0.0187	0.06	10.5	14	7.5	1.86
0.65	0.0187	0.06	19.2	17.9	9.5	1.88
0.41	0.0187	0.06	26.1	27.9	13.2	2.11
0.19	0.0187	0.06	67.1	72.8	32.2	2.26
0.038	0.0187	0.06	77.8	219	66.2	3.30
0.018	0.0187	0.06	79.3	296	68.9	4.29
0.009	0.0187	0.06	84.8	359.1	83.2	4.31

as already mentioned above. While electron transfer from the radical to Cu(II) and a reduction to Cu(I) is a possible mechanism in the case of AIBN initiation, radicals formed by BPO may also coordinate to the copper atoms. In order to understand the nature of the reaction of the initiator with complex **1**, a model reaction of BPO (2 mmol) and **1** (1 mmol) was carried out in a toluene/ethanol solution. The reaction mixture was heated under reflux and stirring for 12 h and rested at room temperature where blue-green crystals were obtained after a few days. The molecular structure of the formed product was established by IR, elemental analysis, and single-crystal X-ray diffraction studies. In the mixture an exchange reaction between the coordinated carboxylates and the BPO radicals occurred, and $Cu_2(OOCC_6H_5)_4 \cdot 2CH_3CH_2OH$ was formed as a product

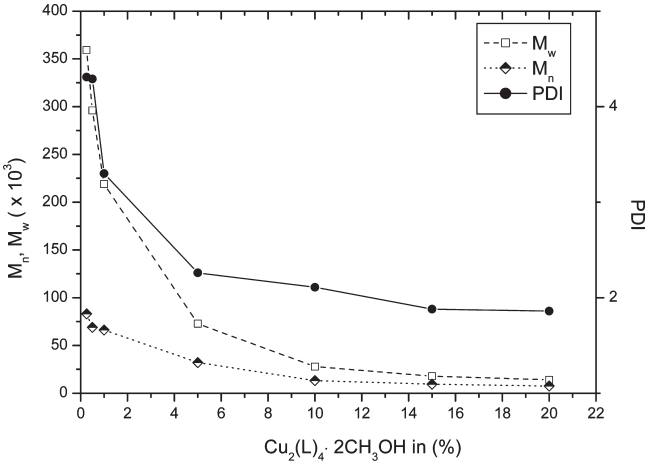

Figure 6. Dependence of M_n, M_w, and PDI on the concentration of $Cu_2(L)_4 \cdot 2CH_3OH$ during radical copolymerization of MMA with $Cu_2(L)_4 \cdot 2CH_3OH$ initiated with AIBN at 85 °C.

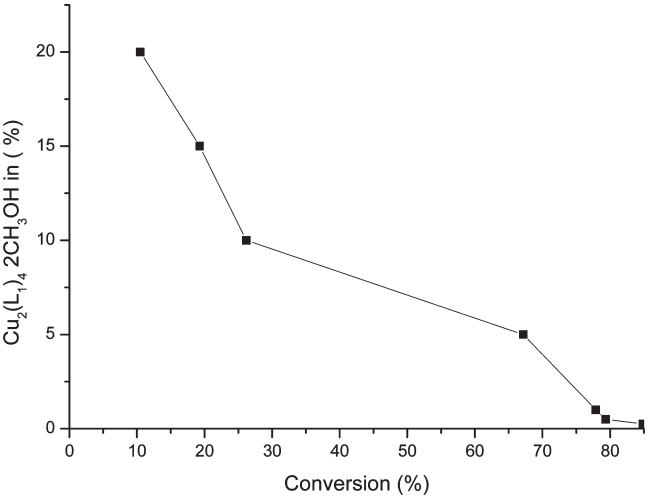

Figure 7. Dependence of conversion on the concentration of $Cu_2(L)_4 \cdot 2CH_3OH$ during radical copolymerization of MMA with $Cu_2(L)_4 \cdot 2CH_3OH$ initiated with AIBN at 85 °C.

(Scheme 4). The resulting complex has a dimeric structure which resembles the structure of **1** (Figure 9). The copper atoms are bridged by four benzoate groups, and the ethanol molecules are bound through their oxygen atoms to the copper atoms. Selected bond distances and angles of

$Cu_2(OOCC_6H_5)_4 \cdot 2CH_3CH_2OH$ are listed in Table 6, and crystal data and structure refinement are summarized in Table 1.

From this model reaction we can conclude that during polymerization primary formed radicals are at least partially consumed by the exchange reaction with the copper complex. Therefore, the concentration of primary radicals decreases at higher concentrations of **1**, and thus the initiation of polymerization is not very effective, which is one reason for lower polymer yields at higher complex concentration. A second mechanism of deactivation of the propagating radicals is the reduction of the Cu(II) center by electron transfer and thus an oxidation of the radical.[25] In the samples with lower concentrations of **1** the exchange reaction will be less prominent, and thus consequently more radicals are able to initiate the polymerization.

The influence of the variation of the initiator concentration on the molecular weight and the conversion was studied using the AIBN initiator (Table 7). In these studies all samples had a constant amount of **1**. The results of copolymerization show that the increase of the concentration of AIBN indicates a higher conversion and a decrease of experimental molecular weights (Figure 10). As explained above, complex **1** inhibits the polymerization deactivating radicals. The samples with higher concentrations of AIBN compensated the deactivated radicals leading to higher conversion. It was observed that reaction mixtures with higher concentrations of AIBN revealed lower molecular weights than those with lower concentration. All obtained polymers

Table 5. Radical Copolymerization of MMA with $Cu_2(L)_4 \cdot 2CH_3OH$ in Bulk Initiated with BPO at 70 °C

$Cu_2(L)_4 \cdot 2CH_3OH$ (mmol)	MMA (mmol)	BPO (mmol)	yield (%)	M_w ($\times 10^3$)	M_n ($\times 10^3$)	PDI
0.95	0.0187	0.082	8.4	12.4	5.91	2.1
0.19	0.0187	0.082	62.6	87.9	28	3.13
0.038	0.0187	0.082	70	269.8	58.9	4.58

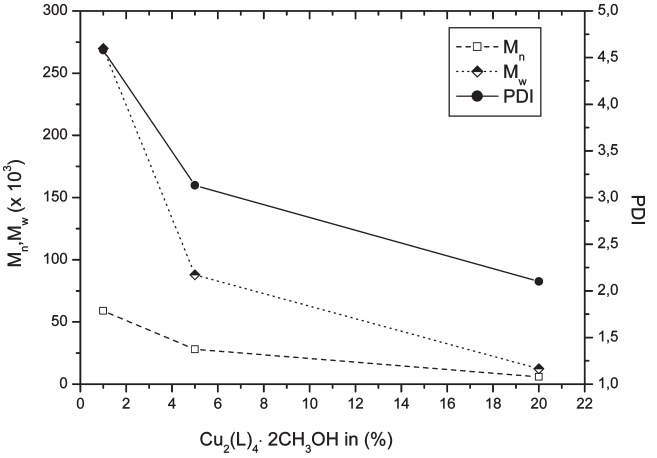

Figure 8. Dependence of M_n, M_w, and PDI on the concentration of $Cu_2(L)_4 \cdot 2CH_3OH$ during radical copolymerization of MMA with $Cu_2(L)_4 \cdot 2CH_3OH$ initiated with BPO at 70 °C.

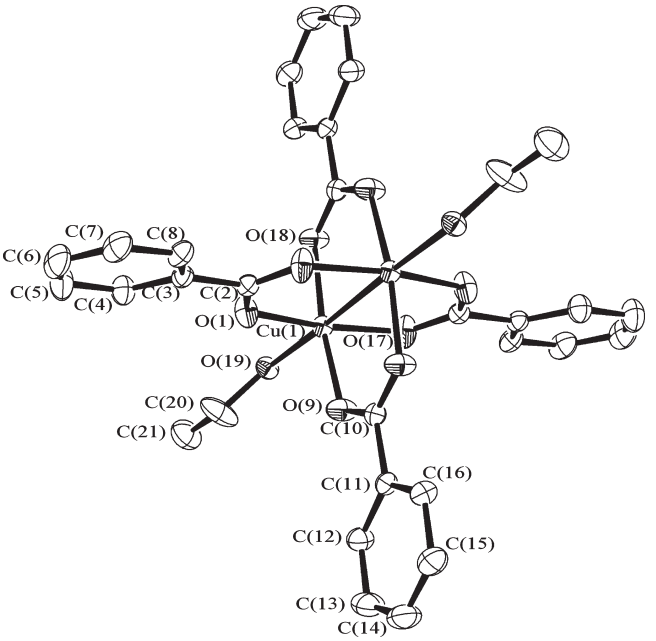

Figure 9. ORTEP view of the molecular structure of $Cu_2(OOCC_6H_5)_4 \cdot 2CH_3CH_2OH$, displaying the thermal ellipsoids at 30% probability. H atoms are omitted for clarity.

Table 6. Selected Bond Lengths [pm] and Angles [deg] for $Cu_2(OOCC_6H_5)_4 \cdot 2CH_3CH_2OH$[a]

Cu(1)−O(1)	194.9(2)	O(17)−Cu(1)−O(9)	89.63(13)
Cu(1)−O(17)	195.0(3)	O(18)−Cu(1)−O(9)	168.96(10)
Cu(1)−O(18)	195.2(2)	O(1)−Cu(1)−O(19)	93.72(12)
Cu(1)−O(9)	196.5(2)	O(17)−Cu(1)−O(19)	97.45(12)
Cu(1)−O(19)	214.7(3)	O(18)−Cu(1)−O(19)	95.61(12)
Cu(1)−Cu(1)#1	258.33(8)	O(9)−Cu(1)−O(19)	95.43(12)
		O(1)−Cu(1)−Cu(1)#1	84.19(7)
O(1)−Cu(1)−O(17)	168.77(10)	O(17)−Cu(1)−Cu(1)#1	84.63(8)
O(1)−Cu(1)−O(18)	88.95(12)	O(18)−Cu(1)−Cu(1)#1	84.09(7)
O(17)−Cu(1)−O(18)	88.84(12)	O(9)−Cu(1)−Cu(1)#1	84.88(7)
O(1)−Cu(1)−O(9)	90.43(13)	O(19)−Cu(1)−Cu(1)#1	177.90(10)

[a] Symmetry transformations used to generate equivalent atoms: #1 $-x + {}^1/_2, -y + {}^3/_2, -z + 1$.

Scheme 4. Synthesis of $Cu_2(OOCC_6H_5)_4 \cdot 2CH_3CH_2OH$

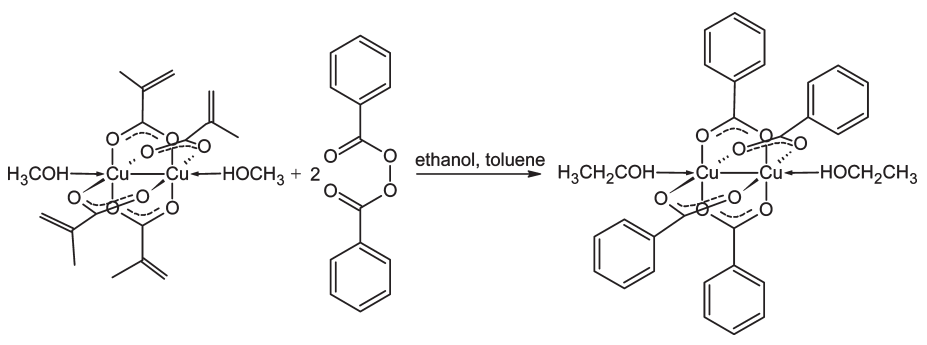

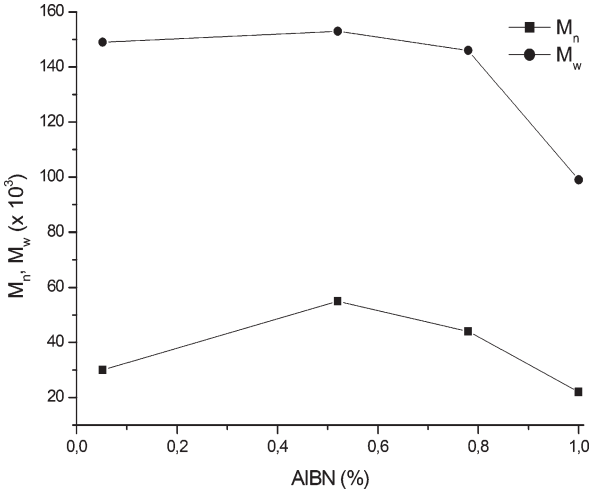

Figure 10. Dependence of M_n and M_w on the concentration of AIBN during radical copolymerization of MMA with $Cu_2(L)_4 \cdot 2CH_3OH$ at 85 °C.

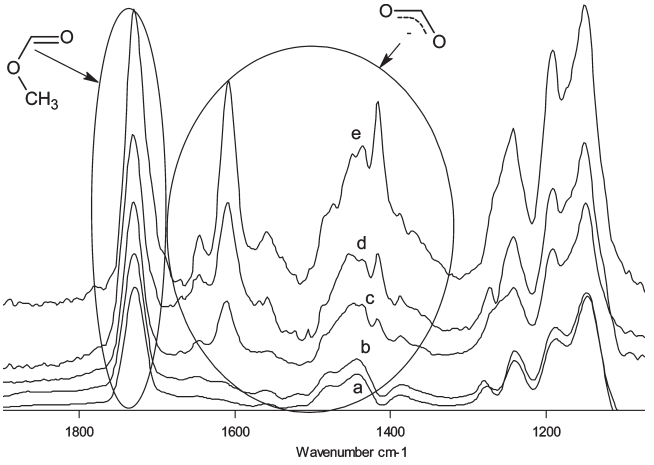

Figure 11. IR spectra of copolymers from MMA with **1**: (a) polymer without complex, (b) copolymer with 0.5%, (c) copolymer with 5%, (d) with 10%, (e) with 20% of **1**.

Table 7. Radical Copolymerization of MMA and $Cu_2(L)_4 \cdot 2CH_3OH$ with Variation of Initiator Concentration at 85 °C

$Cu_2(L)_4 \cdot 2CH_3OH$ (mmol)	MMA (mmol)	AIBN (mmol)	yield (%)	M_w ($\times 10^3$)	M_n ($\times 10^3$)	PDI
0.037	0.0187	0.12	83.6	99	22.7	4.3
0.037	0.0187	0.09	77.8	146	44	3.2
0.037	0.0187	0.06	66.8	153.4	55	4.9
0.037	0.0187	0.006	55.7	149.8	30.5	3.5

were soluble in THF, which means that the degree of cross-linking was low.

The IR spectra of copolymers from MMA with **1** show an absorption at 1609 cm^{-1} that corresponds to the $\nu_{as}(COO^-)$ vibration and another one at 1416 cm^{-1} which attributes to the $\nu_s(COO^-)$ stretching vibration (Figure 11). The separation between $\nu_{as}(COO^-)$ and $\nu_{as}(COO^-)$ for all copolymers is 193 cm^{-1}, indicating a bidentate coordination mode for coordinated carboxylate groups. This reveals that the copper(II) carboxylates incorporated in the polymer have maintained the bidentate coordination mode. The peaks corresponding to $\nu_{as}(COO^-)$ and $\nu_{as}(COO^-)$ are more intense for the samples with higher concentration of **1** which exhibit that these samples have a higher amount of **1** incorporated into the copolymer. The peak at 1729 cm^{-1} corresponds to (COO) stretching from methyl carboxylate group, and the peak at 1646 cm^{-1} to double bonds from **1**.

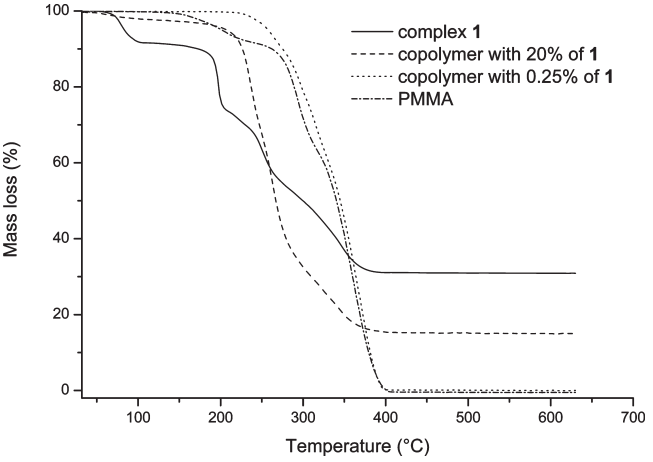

Figure 12. Thermogravimetric analysis of copper(II) complex **1**, copolymer with 20% of **1**, copolymer with 0.25% of **1**, and MMA.

Thermogravimetric Analysis (TGA) of the Copolymers. Some of the factors that have observable effects in the degradation process of copolymers are their molecular mass, cross-linking degree, and the introduction of metal ions or metal clusters in the polymer matrix. Therefore, the thermal stability of the formed copolymers was investigated by heating each sample under an oxygen atmosphere and comparing the results with those of pure PMMA and pure complex **1**. TGA of the pristine complex **1** (Figure 12) shows a first mass reduction at a temperature of 70 °C, which is most likely due to the release of the methanol ligands. The other steps between 190 and 325 °C are based on the decomposition of the carboxylate ligands.[23] TGA of the copolymer with 20% of **1** exhibits three weight-loss steps at 223, 257, and 348 °C and exhibits a higher thermal stability as compared to **1**. The higher decomposition temperature of the copolymer with 20% of **1** compared to complex **1** is most likely due to the incorporation of **1** in the polymer matrix through the formation of covalent bonds. PMMA is more stable than the copolymer with 20% of **1**, which is most likely based on the interaction of **1** with the matrix in the copolymer. TGA of the copolymer with 0.25% of **1** exhibits also three weight-loss steps at 240, 291, and 348 °C, respectively. Literature known examples of copper-containing polymers showed that the introduction of Cu ions lowered the thermal stability of the polymers and led to a stepwise decomposition.[24] The copolymer with 0.25% of complex **1** seems to have higher thermal stability compared to other samples, which is most likely due to cross-linking or the higher molecular weight of this sample.

Collectively, these experimental results suggest that the copolymers are slightly cross-linked or non-cross-linked, and generally an increasing amount of **1** in the reaction mixture produces lower molecular weights. Complex **1** at higher concentrations most likely inhibits polymerization by deactivation of radicals from the propagating chain. The behavior of copolymerization initiated with BPO does not differ significantly from copolymerization initiated with AIBN, and the increase of the concentration of initiator does not result in the formation of cross-linking sites. If we take in consideration the obtained results, we can conclude that the complex **1** reacts during copolymerization with radicals and makes a major contribution to the observed

termination process. Copper(II) carboxylates bearing polymerizable groups have two attractive positions for reaction with radicals: the position at the copper(II) center[25,26] and the double bonds. If radicals react with double bonds from **1**, propagation will not be inhibited. Therefore, the inhibition of polymerization occurs from the reaction of radicals with copper(II) centers. The reaction of copper(II) acetate with alkyl radicals has been previously studied, and a reaction mechanism was proposed.[25] The authors suggested a reduction of copper(II) to copper(I) through the reaction with alky radicals and also oxidation of alkyl radicals. The affinity of copper to react with radicals is the most important circumstance that makes copolymerizations of MMA with **1** having a different behavior compared with other metal complexes that show more stable oxidation states. Copper(II) complexes are catalysts in reverse ATRP together with AIBN as initiator. The proposed reaction mechanism suggests that the primary radicals react reversibly with copper(II) reducing it to copper(I).[27] While in reverse ATRP the Cu(I) species is again able to activate a dormant chain end in our studies only termination reactions are possible. On the basis of the SEC, IR, TGA, single-crystal X-ray analysis, and the reaction mechanisms proposed before, a possible copolymerization mechanism for our system was proposed as shown in Schemes 5, 6, 7, and 8.

Scheme 5. Possible Reaction Mechanism of Primary Radicals with 1[a]

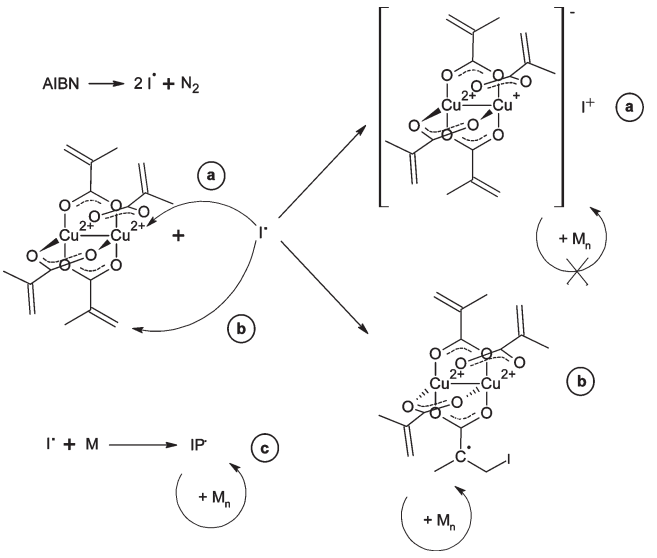

[a] Axial ligands were omitting for clarity.

Scheme 6. Possible Reaction Mechanism of Propagation Radicals with 1[a]

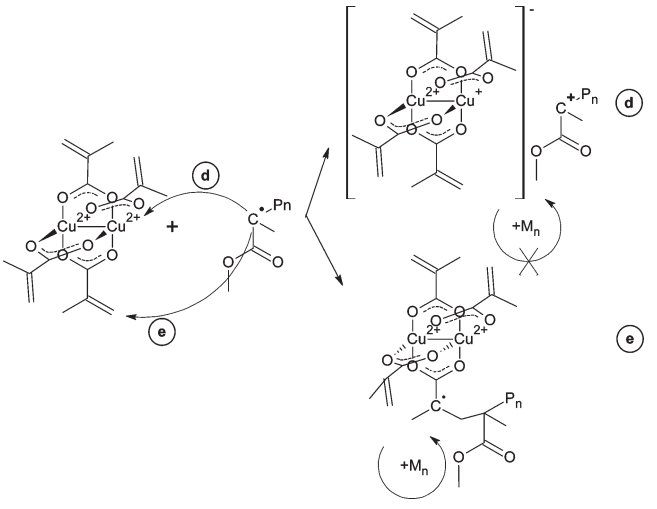

[a] Axial ligands were omitting for clarity.

Possible Reaction Mechanism. In the initiation step, the initiating radicals $\mathbf{I}^{\bullet}$ derived from the decomposition of AIBN can be (a) oxidized to the cation by electron transfer to copper(II), (b) incorporated into double bonds from bridging methacrylates generating a propagating radical directly from copper(II) carboxylate, or (c) react with the double bond causing polymer propagation (Scheme 5). The radicals from propagating chains formed after initiation can react with the complexes via similar mechanisms as the initiators, i.e. (d) reducing copper(II) by electron transfer, or (e) they can initiate further polymerization by reaction with the methacrylate groups (Scheme 6). Loss of a proton from the cation would result in the formation of double bonds (Scheme 7).[28] The cation can also react with a methacrylate anion of a copper(II) complex forming the corresponding coupling product (Scheme 8).

Copolymerization of MMA with **2** using BPO as initiator was carried out applying the same procedure as in the case of AIBN. Complex **2** as compared to complex **1** has a

Scheme 7. Possible Reaction for the Formation of Double Bonds from 1[a]

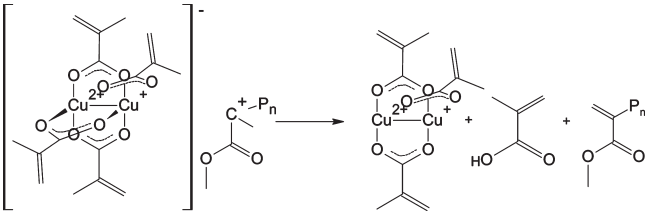

[a] Axial ligands were omitting for clarity.

Scheme 8. Formation of Coupling Product[a]

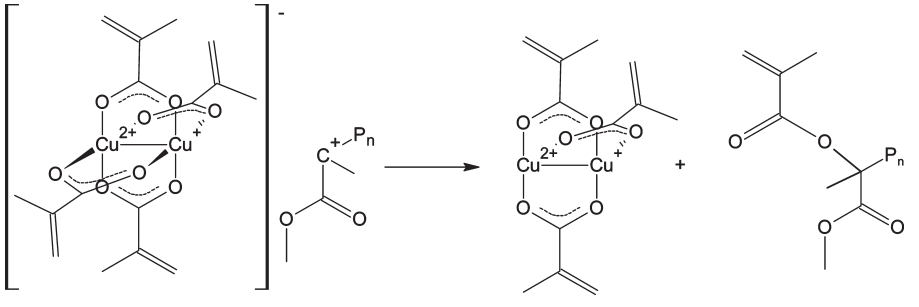

[a] Axial ligands were omitting for clarity.

Table 8. Radical Copolymerization of MMA and $Cu(L)_2 \cdot 2pyridine \cdot 3H_2O$ in Bulk Initiated with BPO at 75 °C

$Cu(L)_2 \cdot 2pyridine \cdot 3H_2O$ (mmol)	MMA (mmol)	BPO (mmol)	yield (%)	M_w ($\times 10^3$)	M_n ($\times 10^3$)	PDI
1.17	0.0187	0.082	15.5	14	6	2.33
0.51	0.0187	0.082	21.4	19.1	7.7	2.48
0.234	0.0187	0.082	45.9	381	15	2.54
0.046	0.0187	0.082	83.1	79.1	21	3.76
0.023	0.0187	0.082	86.2	111.3	31.9	3.48
0.011	0.0187	0.082	89.6	162.1	41.8	3.87

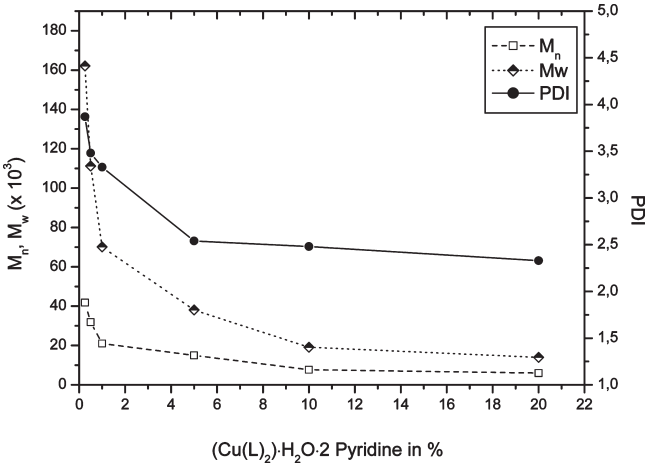

Figure 13. Dependence of M_n, M_w, and PDI on the concentration of $Cu(L)_2 \cdot 2pyridine \cdot 3H_2O$ during radical copolymerization of MMA with $Cu(L)_2 \cdot 2pyridine \cdot 3H_2O$ initiated with BPO at 75 °C.

monomeric structure (Figure 3). Therefore, it was investigated whether this modified complex is able to perform changes in the behavior of copolymerization. Copolymerization of MMA with **2** was carried out in different concentrations using BPO as initiator (Table 8). The polymerization was stopped after heating at 75 °C for 12 h. Residual non-polymerized copper(II) carboxylates and MMA were removed in the same way as described above. Copolymerization of MMA with **2** leads to soluble copolymers, and molecular weights of the copolymers decrease with an increasing concentration of **2** in the reaction mixture (Figure 13). Also, the conversion decreases with increasing concentration of **2.** The samples with 1.17 and 0.51 mmol of **2** do not reach the gelation point. Hence, we can conclude that the behavior of copolymerization of **2** with MMA does not differ significantly from copolymerization of **1** with MMA.

Conclusion

Metal-containing PMMA copolymers were prepared through the radical polymerization of **1** and **2** with MMA using AIBN as well as BPO as initiators. All copolymers prepared are soluble, which is a strong hint that the degree of cross-linking of the polymers is low. Generally, increasing the amount of **1** or **2** in the reaction mixtures produces copolymers with lower molecular weights. The behavior of copolymerization initiated with BPO does not differ significantly from copolymerization initiated with AIBN. Furthermore, copolymerization of **2** with MMA does not differ significantly from copolymerization of **1**. The complexes **1** and **2** at higher concentration inhibit polymerization, appearing to deactivate radicals from propagating chains. Copper(II) carboxylates bearing polymerizable groups have two attractive positions for reaction with radicals: the position at the copper(II) center and the double bonds. If radicals react with double bonds from the complex, chain propagation will occur while generated and the inhibition of polymerization takes place in the reaction of radicals with copper(II) centers. A possible reaction mechanism was proposed.

Acknowledgment. Financial support of this work by the Austrian Fonds zur Förderung der wissenschaftlichen Forschung (FWF, Project nr.: P17424) is gratefully acknowledged.

References and Notes

(1) Kickelbick, G. *Prog. Polym. Sci.* **2002**, *28*, 83–114.
(2) Leonowicz, M. K.; Lawecka, M.; Slawska-waniewska, A.; Dzhardimalieva, G. I.; Rozenberg, A. S.; Pomogailo, A. D. *Macromol. Symp.* **2003**, *204*, 257–265.
(3) Rakhimov, R. R.; Arrington, S. A.; Hwang, J. S.; Prokof'ev, A. I.; Alexandrov, I. A.; Aleksandrov, A. I. *J. Appl. Phys.* **2006**, *99*, 08P904/1–08P904/3.
(4) Zamborini, F. P.; Leopold, M. C.; Hicks, J. F.; Kulesza, P. J.; Malik, M. A.; Murray, R. W. *J. Am. Chem. Soc.* **2002**, *124*, 8958–8964.
(5) Rojas, O.; Araya, M.; Montero, M. L.; Azofeifa, D. E.; Vargas, W. E. *J. Mater. Sci.* **2007**, *42*, 3161–3166.
(6) Lee, L.-H.; Chen, W.-C. *Chem. Mater.* **2001**, *13*, 1137–1142.
(7) Wang, L.-H.; Wang, W.; Zhang, W.-G.; Kang, E.-T.; Huang, W. *Chem. Mater.* **2000**, *12*, 2212–2218.
(8) Ivanovici, S.; Peterlik, H.; Feldgitscher, C.; Puchberger, M.; Kickelbick, G. *Macromolecules* **2008**, *41*, 1131–1139.
(9) Kogler, F. R.; Koch, T.; Peterlik, H.; Seidler, S.; Schubert, U. *J. Polym. Sci., Part B: Polym. Phys.* **2007**, *45*, 2215–2231.
(10) Wang, S.; Zhang, R. *Microchim. Acta* **2006**, *154*, 73–80.
(11) Jezierska, J.; Trochimczuk, A. W.; Kedzierska, J. *Polymer* **1999**, *40*, 3611–3616.
(12) Belfiore, L. A.; Pires, A. T. N.; Wang, Y.; Graham, H.; Ueda, E. *Macromolecules* **1992**, *25*, 1411–19.
(13) Kamigaito, M.; Ando, T.; Sawamoto, M. *Chem. Rev.* **2001**, *101*, 3689–3745.
(14) Kogler, F. R.; Schubert, U. *Polymer* **2007**, *48*, 4990–4995.
(15) Edmondson, B. J.; Lever, A. B. P. *Inorg. Chem.* **1965**, *4*, 1608–12.
(16) Deacon, G. B.; Phillips, R. J. *Coord. Chem. Rev.* **1980**, *33*, 227–50.
(17) Kuz'mina, N. E.; Palkina, K. K.; Polyakova, N. V.; Strashnova, S. B.; Koval'chukova, O. V.; Zaitsev, B. E.; Levov, A. N. *Russ. J. Coord. Chem.* **2001**, *27*, 711–716.
(18) Van Niekerk, J. N.; Schoening, F. R. L. *Acta Crystallogr.* **1953**, *6*, 227–32.
(19) Petric, M.; Leban, I.; Segedin, P. *Polyhedron* **1995**, *14*, 983–9.
(20) Uruska, I.; Stefanczyk, I. *J. Chem. Eng. Data* **1991**, *36*, 359–60.
(21) Baggio, R.; Foxman, B.; Garland, M. T.; Perec, M.; Shang, W. *Acta Crystallogr., Sect. C: Cryst. Struct. Commun.* **2000**, *C56*, E505–E506.
(22) Zhu, S. M.; Wang, W. X.; Tu, W. P.; Yan, D. Y. *Acta Polym.* **1999**, *50*, 267–269.
(23) Czakis-Sulikowska, D.; Radwanska-Doczekalska, J.; Czylkowska, A.; Goluchowska, J. *J. Therm. Anal. Calorim.* **2004**, *78*, 501–511.
(24) Von Lampe, I.; Brueckner, A.; Goetze, S. *Angew. Makromol. Chem.* **1997**, *251*, 157–170.
(25) Jenkins, C. L.; Kochi, J. K. *J. Am. Chem. Soc.* **1972**, *94*, 843–55.
(26) Jenkins, C. L.; Kochi, J. K. *J. Am. Chem. Soc.* **1972**, *94*, 856–65.
(27) Matyjaszewski, K.; Xia, J. *Chem. Rev.* **2001**, *101*, 2921–2990.
(28) Matyjaszewski, K.; Wei, M.; Xia, J.; Gaynor, S. G. *Macromol. Chem. Phys.* **1998**, *199*, 2289–2292.